Preliminary Design Calculation of Stress Corrosion Cracking (SCC) Machine

Y. Amalia, A.Sudiyanto, F.Rahmawati, S.U.Santoso, Z.N.Y.Pratama, E. Pujiyulianto

Universitas Pembangunan Nasional Veteran Yogyakarta
E-mail address ekopuji39@gmail.com

Abstract

This research aims to evaluate the design calculation of stress corrosion cracking (SCC) machine. The design calculation was based on the specimen standard of SCC in the constant load set up for Aluminum alloys by using mechanics material principles. The results of the design calculation show that the minimum radius horizontal material support, horizontal walking support, and horizontal load support were 8.50, 9.73, and 6.7 mm that is made of steel, respectively. The minimum radius of specimen support and the load support is 3.2 mm that is made of steel and 1.75 mm that is made of stainless steel, respectively. The height of the walking load support in the center must be higher than the height of the walking load support in the corner as per moment calculation.

Keywords: Design calculation, Stress Corrosion Cracking (SCC), Mechanics Material, Aluminum alloys.

I. INTRODUCTION

Metal is one of the main materials used in daily life (Hamann & Hamann, 2018) and industry i.e. mining, aerospace, transportation, fabrication, manufacture, heat exchanger, building, and construction (Robert, 2020), etc. Besides the number of uses of metals, metals have a major problem in their resistance to corrosion failure (Popoola, et al., 2013). Corrosion is the degradation of materials caused by interactions between them and the environment (Cwalina, 2014). The common types of corrosion are galvanic corrosion, crevice corrosion, pitting corrosion, microbiological corrosion, and stress corrosion cracking (SCC). Stress corrosion cracking (SCC) is a case of intergranular or transgranular cracking due to the combined effect of stress and a corrosive environment that can cause a failure in metal and alloy components (Dietzel & Srinivasan, 2011). Several components that often fail due to stress corrosion cracking are components in the mining, oil, gas, infrastructure, and chemical industries such as boilers, turbine blades (Shen, et al., 2019), power plants, cable bolts (Wu, et al., 2018), pipe (Rao, et al, 2018), and heat exchangers.

The failure mechanisms due to stress corrosion cracking (SCC) have three main stages (Rao, et al., 2016). The first stage is starting with the initial crack appearance stage, the second stage is the crack propagation stage, and the final stage is a failure. The three stages in the failure process occur continuously.

The failure due to stress corrosion cracking (SCC) is very detrimental and should be avoided because it tends to be catastrophic (Geissler, et al., 2019). It cannot be predicted due to a significant reduction in resistance to stress below its normal fracture stress, therefore the SCC is very dangerous and needs more cost to repair and replace the failed components. The theoretical approaches are very important to understand the mechanisms, phenomena, and causes of stress corrosion cracking (SCC), so that an idea to understand the mechanisms, phenomena, and causes of stress corrosion cracking (SCC) is by making the stress corrosion cracking (SCC) machine. Before going to make and to manufacture the SCC machine, the preliminary design calculation should be conducted to know the proper size and shape, thus the failure on each part in the stress corrosion cracking (SCC) machine can be prevented. Some part on the stress corrosion cracking (SCC) machine has the potential to experience failures, such as walking support, horizontal walking support, horizontal material support, material support, horizontal load support, and load support, therefore this study aims to determine the size and shape of walking support, horizontal walking support, horizontal material support, material support, horizontal load support, and load support to obtain a safe size and shape.

II. RESEARCH METHODOLOGY

The design of stress corrosion cracking (SCC) was shown in Fig. 1a. The design was used for the constant load Stress Corrosion Cracking (SCC) process for aluminum alloys. The main parts that were considered in the calculation were the shape of the walking support, the minimum diameter of the horizontal walking support, horizontal material support, material support, horizontal load support, and load support as indicated in Fig. 1b. The calculation was based on the gauge length specimen standard of SCC in the constant load set up. The specimen's standard of SCC was shown in Fig.2.

(a)

(b)
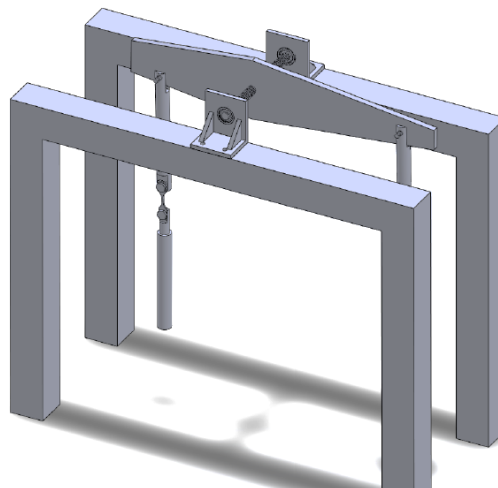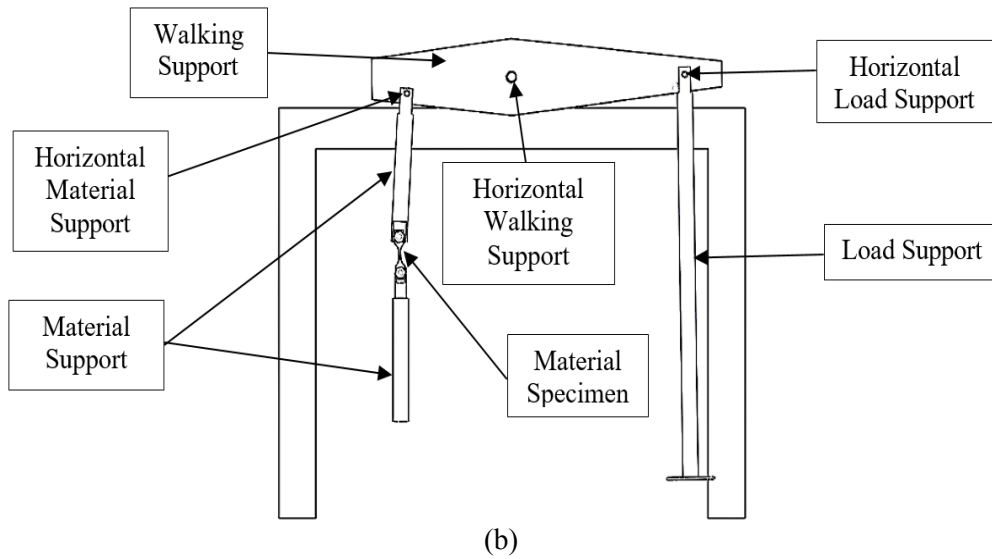
Figure 1. Design of SCC machine: a) The assembly design of the SCC machine and b) the main part in the SCC machine.
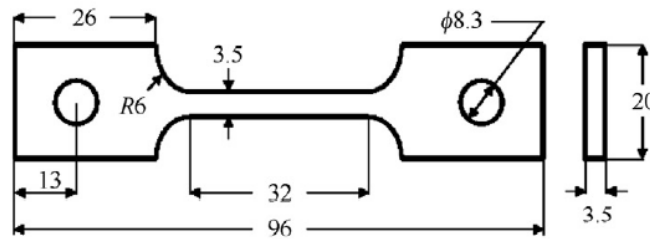
Figure 2. Specimens standard of SCC (Kumar, et al., 2015)

The materials that were used for walking support, the horizontal walking support, horizontal material support, horizontal load support, and load support were steel, and the material for material support was stainless steel.

The mechanics material principles such as the uniaxial strength and three-point bending equations were used in the calculation to get the proper shape of walking support, and the minimum radius of the horizontal walking support, horizontal material support, material support, horizontal load support, and load support. the uniaxial strength and three-point bending equations were shown in Eq.s 1 and 2, respectively.

$$\sigma = \frac{F}{A} \quad \dots\dots\dots\dots\dots\dots\dots\dots\dots\dots\dots\dots\dots\dots\dots\dots\dots\dots\dots\dots\dots\dots\dots 1$$

$$\sigma = \frac{F\ L}{\pi\ R^3} \quad \dots\dots\dots\dots\dots\dots\dots\dots\dots\dots\dots\dots\dots\dots\dots\dots\dots\dots\dots\dots\dots 2$$

The σ is the stress (kgf/mm2), F is the force (kgf), A is Area (mm2), L is the distance support (mm), R is the radius of the rod for each support (mm). The minimum size on each part was used as the minimum standard size on each part in the machine without using the safety factor. Besides the

uniaxial strength and the three-point bending calculation, the bending moment was used for considering the moment distribution in the walking support. The moment Eq. was expressed in the Eq. 3. Where the M is Moment (kgf.mm), and l is the distance of the support (mm).

$$M = F \ x \ l ....3$$

III. FINDING AND DISCUSSION

The load of SCC is operated under the yield strength of the specimens. The used specimens are aluminum alloy, and the yield strength of the aluminum alloy is 28.144 kgf/mm2 (ASM, 2020). By considering the specimen's size in gauge length as shown in Fig. 2, then the surface area of the specimen is 12.25 mm2. Eq. 1 is used to know the maximum load in the yield strength condition of the specimen. By using Eq. 1, the maximum load (F_{max}) is 344.764 kgf. The maximum load is used as the reference load of the structure. The structure is simplified to be a free body diagram as shown in Fig. 3
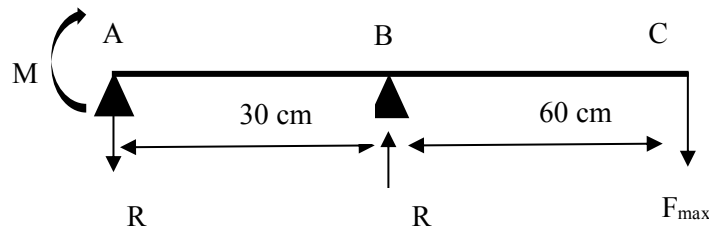
Figure 3. Free Body Diagram of the Structure

The RA and RB as shown in Fig. 3 are calculated by using Eq. 3. From the calculation, the RA and RB are 689.528 kgf and 1034.28 kgf. The maximum moment (M_{max}) in Fig. 3 is 310284 kgf.mm. The moment is calculated by using Eq. 3. The Moment diagram for the structure is shown in Fig. 4. The moment diagram can be used to predict the deflection of the structure, or it can be used to predict the shape of the structure. From Fig. 4. It can be concluded that the height of walking load support in the center (point B) must be higher than the height of the walking load support in the corner (point A) as per the moment diagram in Fig. 4. The reason is due to the maximum moment is occurred in the center of the walking support structure (point B).
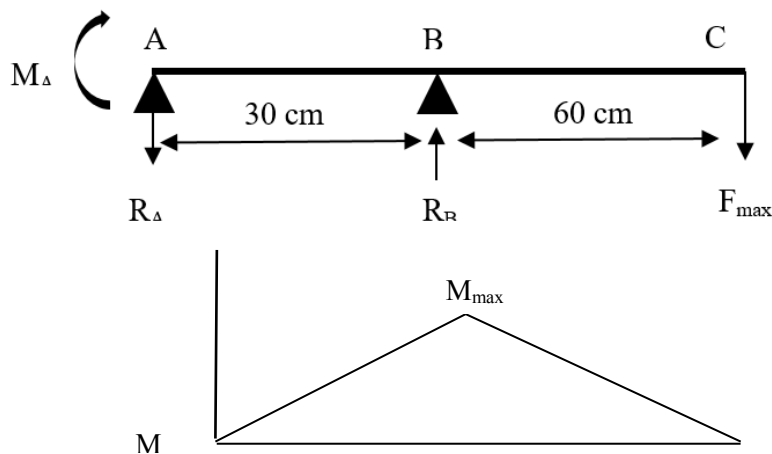
Figure 4. Moment Diagram

The RA and RB as explained earlier are used to calculate the minimum radius of the rod that is used for horizontal material support, horizontal walking support, and horizontal load support. The case for horizontal material support, horizontal walking support, and horizontal load support is three-point bending, and the free-body diagrams for each part are shown below in Fig. 5.

(a)

(b)

(c)
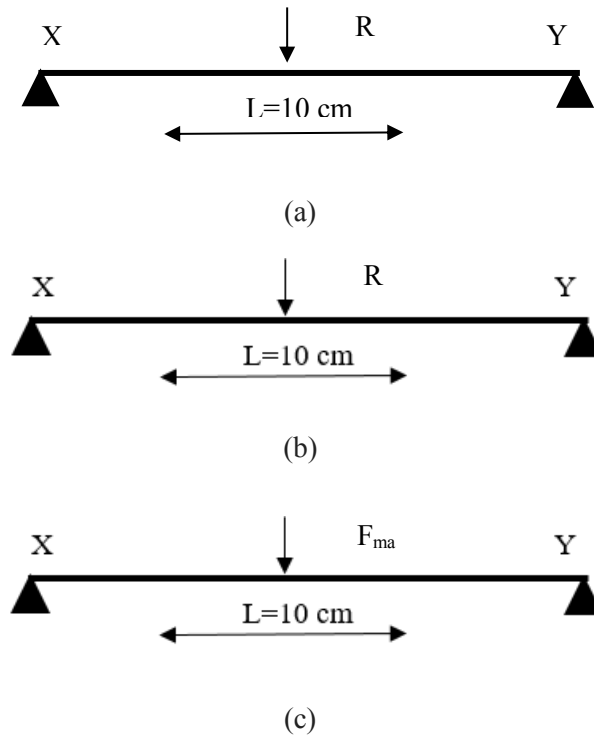
Figure 4. Free body diagram of three-point bending: a) horizontal material support, b) horizontal walking support, and c) horizontal load support.

The Eq. 2 is modified to know the minimum radius of the rod for horizontal material support, horizontal walking support, and horizontal load support. The modified Eq. 2 is shown below in Eq. 4. The R is the minimum radius of the rod under the yield strength limit of the Aluminum alloys specimens.

$$\sigma = \frac{F\,L}{\pi\,R^3}$$

$$R^3 = \frac{F\,L}{\pi\,\sigma}$$

$$R = \sqrt[3]{\frac{F\,L}{\pi\,\sigma}} \dots\dots\dots\dots\dots\dots\dots\dots\dots\dots\dots\dots\dots\dots\dots(4)$$

From the calculation using Eq. 4, the minimum radius (R) of horizontal material support, horizontal walking support, and horizontal load support are 8.50, 9.73, and 6.75 mm, respectively. The results are shown in Fig. 6. The safety factor is not considered in the calculation. In application, the rod radius of horizontal material support, horizontal walking support, and horizontal load support should be more than 8.50, 9.73, and 6.75 mm, respectively, and the additional radius size is following the used safety factor.
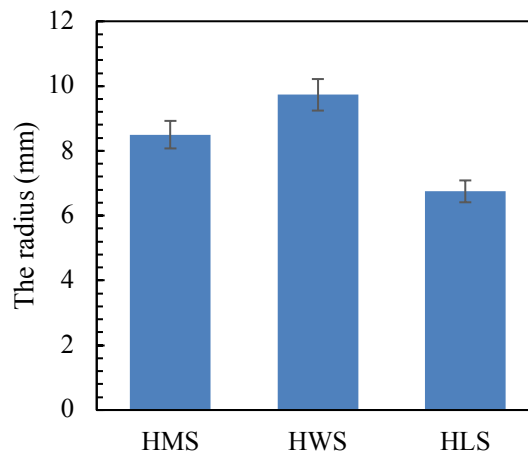
Figure 6. The minimum radius of Horizontal Material Support (HMS), Horizontal Walking Support (HWS), and Horizontal Load Support (HLS).

The Eq. 1 is modified to calculate the minimum radius of material support and load support. The difference in the use of the Eq. for material support and load support other than the horizontal material support, horizontal walking support, and horizontal load support is due to the load received by the material. In the material support and load support, the load is in uniaxial case. The modified Eq.1 is described below in Eq. 5.

$$\sigma = \frac{F}{A}$$

$$\sigma = \frac{F}{\frac{1\pi d^2}{4}}$$

$$d = \sqrt{\frac{4F}{\sigma\pi}}$$

Where: $R = \frac{d}{2}$

$$R = \frac{\sqrt{\frac{4F}{\sigma\pi}}}{2} \dots\dots(5)$$

The calculations using Eq. 5 indicate that the minimum radius (R) of material support and load support are 3.2 and 1.75 mm, respectively. The results are shown in Fig. 7. The difference in the radius is due to the force work on the material are different and the yield strength for each part is

different due to different materials used. The material used for material support is stainless steel and the load support is steel, and The yield strength for each material is 21.29 kgf/mm2 and 35.69 kgf/mm2, respectively. The use of stainless steel in the material support is due to the material on material support will contact directly to the corrosive solution in the experiment, therefore the material might behave good corrosion resistance.
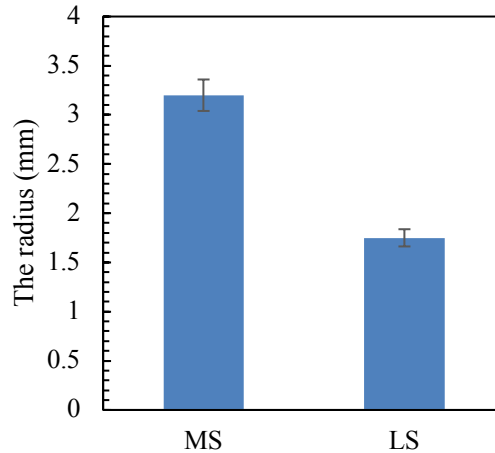
Figure 7. The minimum radius of Material Support (MS) and Load Support (LS).

IV. CONCLUSION

In this research, the preliminary design calculation of stress corrosion cracking (SCC) machine was investigated. Based on the result, it is concluded that the minimum radius horizontal material support, horizontal walking support, and horizontal load support were 8.50, 9.73, and 6.7 mm that is made of steel, respectively. The minimum radius of specimen support and the load support is 3.2 mm that is made of steel and 1.75 mm that is made of stainless steel, respectively. The height of the walking load support in the center must be higher than the height of the walking load support in the corner as per moment calculation.

REFERENCES

Anon., ASM Aerospace Specification Metals Inc. Available at http://asm.matweb.com/search/SpecificMaterial.asp?bassnum=MA6061T6, Accessed 2020.

Cwalina, B., 2014. Biodeterioration of concrete, brick, and other mineral-based building materials. In: T. Liengen, R. Basseguy, D. Feron, and I. B. Beech, 1st eds. Understanding Biocorrosion: Fundamentals and Application: Woodhead Publishing. 281-312.

Dietzel, W., and Srinivasan, P. B., 2011. Testing and evaluation methods for stress corrosion cracking (SCC) in metals. Australia: Woodhead Publishing Limited.

Geissler, D., Uhlemann, M., and Gebert, A., 2019. Catastrophic stress corrosion failure of Zr-base bulk metallic glass through hydrogen embrittlement. *Corrosion Science*, 159, 108057.

Hamann, C. R., and Hamann, D., 2018. Metals in Everyday Life. In: J. T. J.K. Chen, ed. *Metals allergy*: Springer International Publishing, 137-162.

Kumar, M. V., Balasubramanian, V., Rajakumar, S., and Albert, S. K., 2015. Stress Corrosion Cracking Behaviour of Gas Tungsten Asr welded Super Austenitic Stainless Steel Joints. *Defense Technology*, 11, 282-291.

Popoola, L. T. et al., 2013. Corrosion Problems during Oil and Gas Production and Its Mitigation. *International Journal of Industrial Chemistry*, 4 (35), 1-15.

Rao, M. A., Babu, R. S. & Kumar, M. V., 2018. Stress Corrosion Cracking Failure of SS316L High-Pressure Heater Tube. *Engineering Failure Analysis*, 90, 14-22.

Rao, A. C. U., Vasu, V., Govindaraju, M. & Srinadh, K. V. S., 2016. Stress Corrosion Cracking Behaviour of 7xxx Alumunium Alloys: A Literature Review. *Transactions of Nonferrous Metals Society of China*, 26 (6), 1447-1471.

Robert, R., 2020. Metals for Buildings: Essential & Fully Recyclable: International Polar Foundation.

Shen, S. et al., 2019. A Study on Stress Corrosion Cracking and Hydrogen Embrittlement of Jethete M152 Martensitic Stainless Steel. *Material Science and Engineering A*, A740-741, 243-251.

Wu, S. et al., 2018. Investigation of Cable Bolts for Street Corrosion Cracking Failure. *Construction and Building Materials*, 187, 1224-1231.